

# Simply Mechanized Attitude Control for Spinning Vehicles

GEORGE W. LeCOMPTE\*

*Hughes Aircraft Company, Tucson, Ariz.*

AND

JERREL G. BLAND†

*The Boeing Company, Seattle, Wash.*

The two functions required for attitude control of a spinning vehicle, error correction and nutation removal, are accomplished by a single-channel control system. Control torque is applied by a single jet mounted rigidly to the vehicle and producing torque pulses of fixed amplitude and duration when triggered by pulses from a body-mounted passive sensor. The electronics are limited to the sensor amplifier, a fixed time delay, and a solenoid-valve driver. The valve poppet is the only moving part. Proper orientation depends on positioning the sensor and torquing axis at a unique angular separation determined by the ratio of the spin-axis and normal-axis moments of inertia. Analog simulation results show the performance of the control system in aligning the vehicle spin axis to a point or finite-angular-size reference source. A laboratory satellite simulator has also been operated with this control system.

## Introduction

THE attitude stability inherent in a spinning body has led to many applications in missiles, sounding rockets, and satellites. Where the mission requires active control of spin-axis orientation, design of the control system is complicated by the oscillatory nutation motion characteristic of a gyroscope. Control systems incorporating body-fixed attitude sensors and torquing jets have been designed which overcome the nutation problem by open-loop control<sup>1</sup> or with a separate sensor that permits nutation to be measured and controlled.<sup>2</sup>

## System Description

The system discussed here further simplifies control by eliminating the need for independent measurement of the mean attitude error and nutation. As depicted in Fig. 1, the components of the system are a fixed sensor with a spherical field of view, a single torque-producing jet, and electronics consisting of the sensor amplifier, a set time delay, and a valve-driving circuit. Each time that the spinning of the vehicle causes the sensor to scan across the "target" (sun, star, earth, another vehicle, etc.), a torque pulse of fixed duration is triggered. By adjusting the angle between sensor and torquing axes to suit the vehicle's spin-axis-to-normal-axis moment-of-inertia ratio and the delay time to suit the spin rate, this simple system will reduce both the mean attitude error and the nutation. Orientation accuracy is not limited by the angular size of the target but by the precession increment produced by one torque pulse. The sensor is designed with a dead zone that will contain the target with a margin slightly greater than one precession increment. Limit cycle oscillation is prevented by this margin, which determines the maximum steady-state error. Choice of precession increment is determined by the trade between tracking accuracy and acquisition time.

## Behavior of a Spinning Body

The precession and nutation behavior of a spinning body is portrayed in Fig. 2. Initially, the body is assumed to spin

about its principal axis of inertia (spin axis) with an orientation along the vector  $H_0$ , which represents the total angular momentum of the body. The application of an impulsive torque to the body causes the change in angular momentum,  $\Delta H$ . The ensuing motion of the spin axis is a conical nutation about the new angular momentum vector,  $H_1$ . As derived by Azeltine,<sup>3</sup> the response is

$$\phi(t) = (\Delta H/H) \sin \omega_n t$$

$$\theta(t) = \theta_0 - (\Delta H/H)[1 - \cos \omega_n t]$$

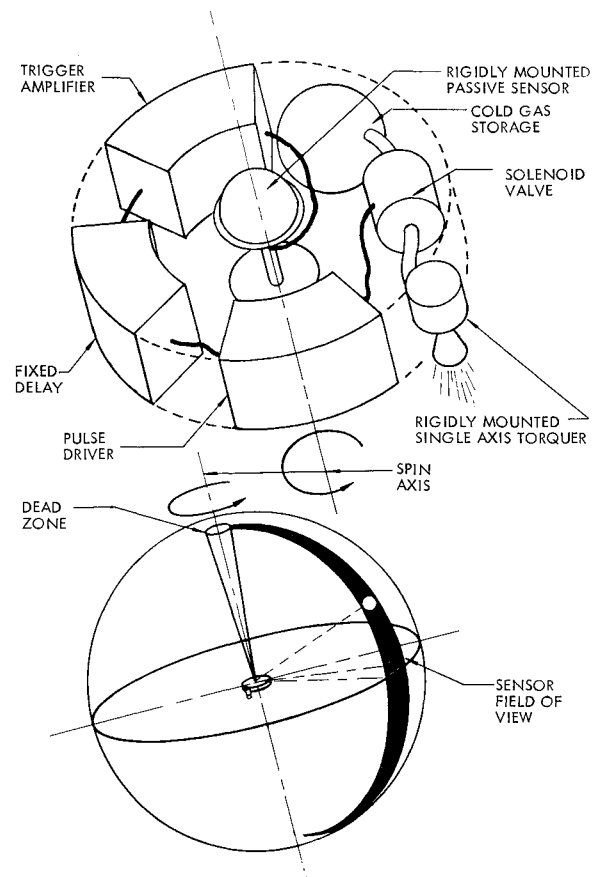


Fig. 1 Control system schematic.

Presented as Preprint 63-341 at the AIAA Guidance and Control Conference, Cambridge, Mass., August 12-14, 1963; revision received July 6, 1964.

\* Senior Staff Engineer.

† Research Engineer. Member AIAA.

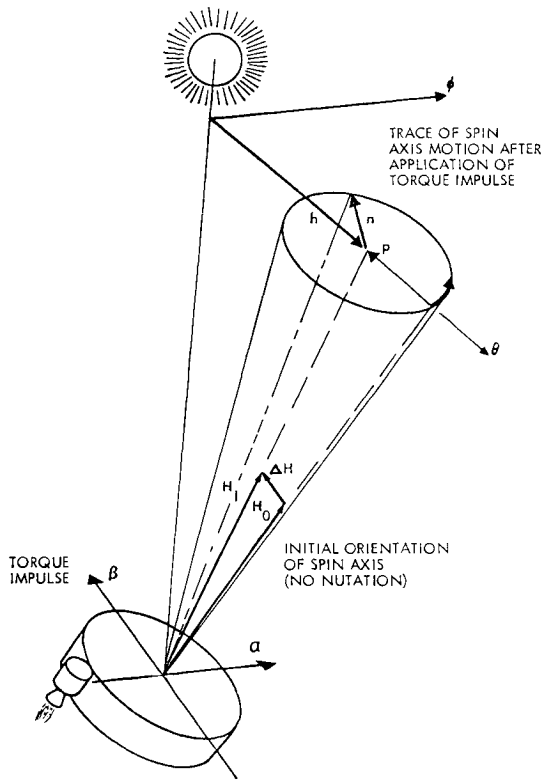


Fig. 2 Spinning body behavior.

where

- $\phi$  and  $\Theta$  = inertially measured displacements of the spin axis from a reference axis (taken as the line of sight to the target)
- $\omega_n$  = nutation angular rate,  $\omega_n = J_s/J_n \omega_s$
- $T\delta\tau$  = torque impulse, oriented opposite the initial displacement,  $\Theta_0$ ,  $T\delta\tau = \Delta H$
- $H$  = angular momentum,  $H = J_s\omega_s$
- $J_s$  = spin axis moment of inertia
- $J_n$  = normal axis moment of inertia
- $\omega_s$  = spin rate
- $(t)$  = time measured from the application of the torque impulse

For this small-angle approximation, the angular motions of the body can be depicted in two dimensions by the trace

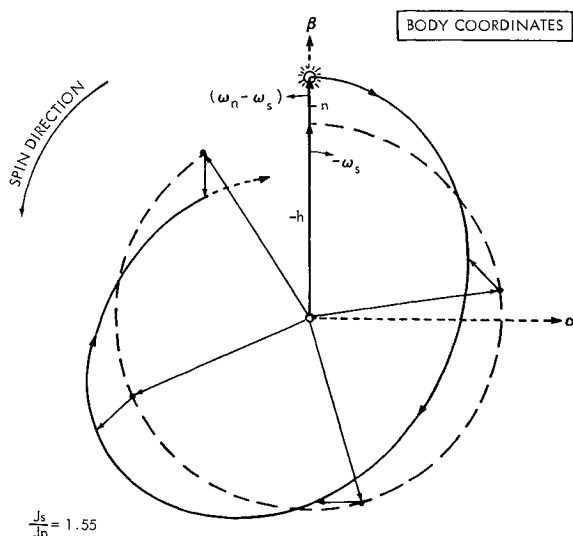


Fig. 3 Apparent target motion in body coordinates.

of the spin axis in a plane a unit distance above the body and normal to the reference axis. As shown in Fig. 2, the trace in this plane can be generated by two vectors: the  $h$  vector, representing the mean attitude error between the angular momentum vector and the reference axis, and the  $n$  vector, which emanates from the tip of the  $h$  vector and revolves at the nutation rate  $\omega_n$ . An instantaneous change in the orientation of the angular momentum vector, due to an impulsive torque, is represented by a change in the vector  $h$ . Because the spin axis cannot change position instantaneously, the change in the vector  $n$  must be equal and opposite to the change in  $h$ . In Fig. 2 a vehicle, originally spinning with no nutation about an axis defined by the angular momentum vector  $H_0$ , has received an impulsive torque normal to the spin axis and in the direction of the desired orientation (line of sight to the sun or other target). The response is depicted in two dimensions by a precession vector  $p$ , tending to reduce the attitude error and leaving a mean attitude error vector  $h$ . The nutation introduced is represented by the revolving vector  $n$ . The  $n$  vector is exactly equal and opposite to the  $p$  vector at the instant of the torque impulse; Fig. 2 shows  $n$  after about 2.5 rad of the nutation cycle.

After one-half cycle of nutation, the  $n$  vector will lie along the  $h$  vector. Application of a second, identical torque impulse at this time will further reduce the mean attitude error and also cancel out the nutation. The angular momentum vector would be two precession increments closer to the target line-of-sight and once again coincident with the vehicle spin axis. To achieve this desirable behavior with a vehicle having a single, rigidly mounted torquer, an odd multiple of half-cycles of nutation must occur during one period of vehicle rotation. Because the  $J_s/J_n$  ratio must lie in the range from zero (slender rod spinning about its axis) to two (thin-disk spinning about a normal axis through its center),  $\frac{1}{2}$  and  $\frac{3}{2}$  are the only physically realizable solutions for a rigid vehicle. In the latter case (flywheel-type vehicle), one and a half nutation cycles occur between torque impulses. Generalizing from Fig. 2, when both mean attitude error and nutation exist, a corrective torque impulse, applied one-half nutation cycle after the time when the  $h$  and  $n$  vectors add in phase, will reduce each of these vectors by one precession increment. These two concepts, inherent nutation cancellation and half-nutation cycle delay, are the key principles behind the simple one-channel attitude control.

### Apparent Target Motion in Body Coordinates

For a control system that is to be rigidly mounted to a spinning vehicle, it is desirable to describe the apparent motion of the target in body coordinates as it is seen by the target sensor. This is accomplished by changing the center of coordinates from the reference axis to the spin axis and rotating the observation plane in synchronism with the spinning vehicle. Mean attitude error thus appears as  $-h$ , rotating opposite the vehicle spin direction at the rate  $-\omega_s$ . The nutation vector is also reversed to a  $-n$ , and rotates at the difference frequency  $\omega_n - \omega_s$ . For bodies rotating about an axis of maximum moment of inertia, these vectors rotate in opposite directions, as depicted in Fig. 3. For the condition shown where the dominant vector is the mean attitude error, nutation appears as a perturbation of the target image trace from the circular motion due to just the mean target error. With increasing nutation amplitude, the target image trace takes on lobed characteristics as shown in Fig. 4a. The three-lobed pattern shown is characteristic of bodies with moment of inertia ratios near 1.5.

The direction of rotation of the target image about the spin axis is determined by the relative magnitude of the mean attitude error and the nutation amplitude. The direction of rotation of the target image in Fig. 4a, where the mean target error dominates, is opposite to the direction of spin. Figure 4b depicts a condition where the nutation amplitude

dominates and the target image rotates about the spin axis in the spin direction. As the ratio of nutation amplitude to mean attitude error increases further, the trace of the target image approaches a circular pattern at the difference frequency  $\omega_n - \omega_s$  with a radius equal to the nutation amplitude.

Each of the circular patterns resulting from the two extreme ratios of nutation amplitude to mean target error represents ideal conditions for one of the two operating modes of the control system.

### Principle of Operation

#### Control Modes

Conceptually, the control system has two modes: one for correction of mean attitude error and one for nutation reduction. Figure 5 depicts these two idealized control modes. As shown in body coordinates, the sensor axis is displaced from the torque axis by an angle equal to the vehicle's rotation during one-half of one nutation cycle. Thus, in Fig. 5a, where a pure mean attitude error is assumed (no nutation), the target appears to move from the sensor axis to the torque axis during the half-nutation cycle delay period, so that the precession increment is toward the target, reducing the mean attitude error and introducing nutation. When a finite duration torque pulse is used, the electrical delay is reduced by half the pulse duration, so that the net precession is in the desired direction.

In Fig. 5b, a pure nutation case is assumed (angular momentum vector coincident with the line of sight to the target), and the apparent target motion is reversed. During the half-nutation cycle delay time, the target moves in the direction of vehicle spin at the difference rate  $\omega_n - \omega_s$ . Thus, when the correction is applied, the target is displaced from the torque axis by the sum of the sensor displacement  $\omega_s t_d$ , and the apparent rotation due to nutation  $(\omega_n - \omega_s)t_d$ . This sum,  $\omega_n t_d$ , is exactly  $180^\circ$  if the delay time  $t_d$  is made equal

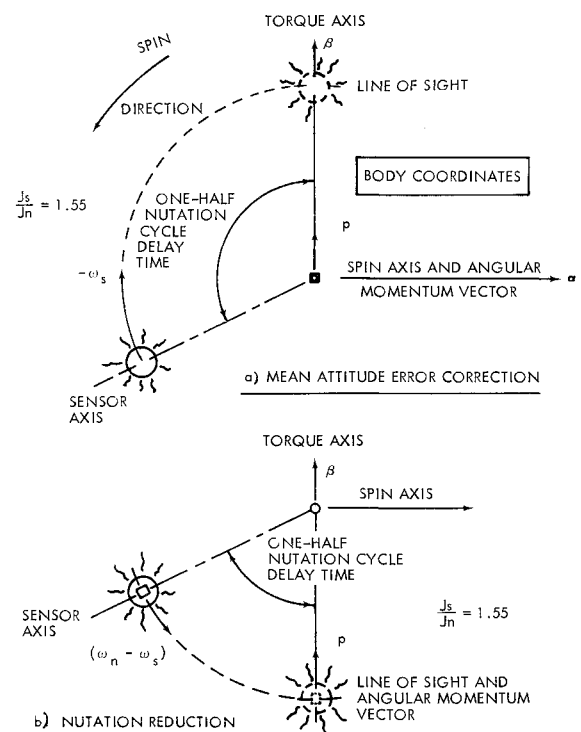


Fig. 5 Control system operating modes.

to one-half of one nutation cycle. This results, as shown in Fig. 5b, in the precession increment reducing the magnitude of the nutation and introducing a mean attitude error.

The same idealized situations are shown in inertial coordinates in Fig. 6 as an aid to visualizing system operation. The mean attitude error correction mode shows the vehicle spin motion during the delay as being equal to the displacement of the sensor axis ahead of the torque axis. In Fig.

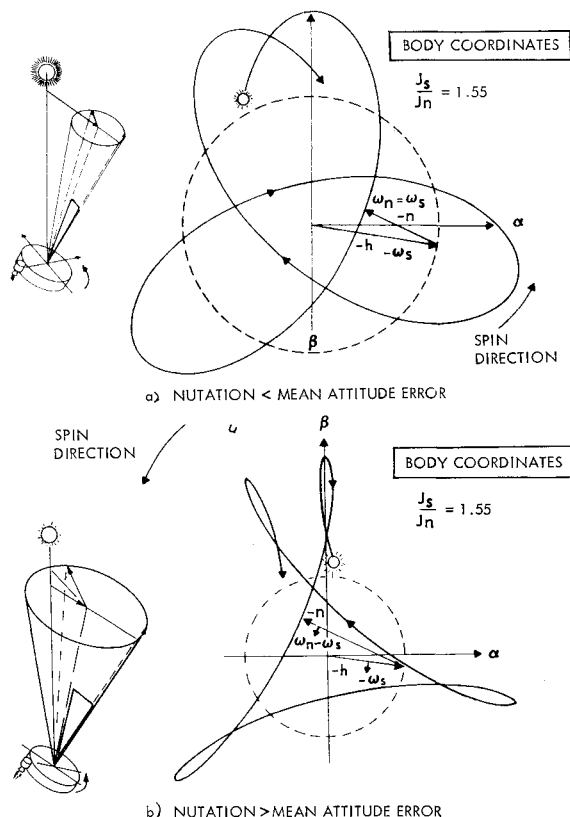


Fig. 4 Effect of nutation on apparent target motion.

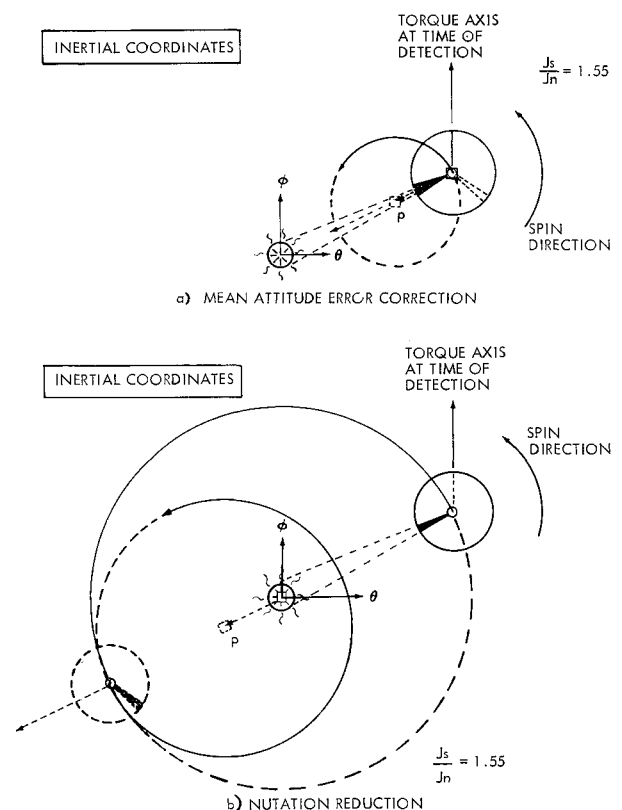


Fig. 6 Operating modes in inertial coordinates.

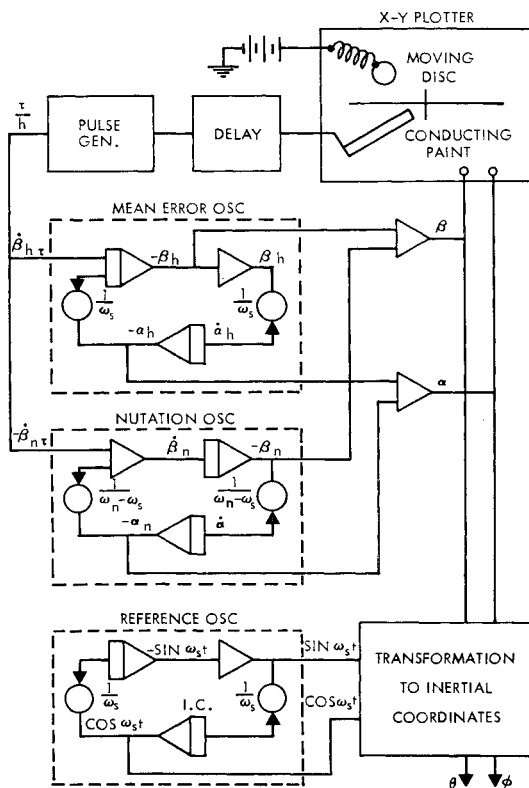


Fig. 7 Spinning vehicle simulation in body coordinates.

6b, the instantaneous spin axis orientation at the time of target detection is exactly the same as in Fig. 6a, but the nutation motion carries the spin axis to the opposite side of the target during the delay time. Thus, the torque axis in this case is pointed away from the target when the precession increment is applied and the angular momentum vector (assumed coincident with the line of sight to the target) is precessed toward the spin axis, reducing the nutation amplitude.

#### Moment-of-Inertia Considerations

The choice of a body moment-of-inertia ratio near 1.5 is determined by the behavior during acquisition, when a large error correction is made, by pulsing the torquer during every revolution. With a nutation rate 1.5 times the spin rate, the nutation introduced during one revolution is  $180^\circ$  out of phase with that from the preceding pulse, and a large build-up of nutation is avoided. Figures 3 and 4 show patterns of apparent target motion for three typical conditions of combined error and nutation. The figures are drawn for a nutation rate 1.55 times the spin rate. Note that, if the ratio were exactly 1.5, the patterns would be repeating three-lobed figures. In the situations of Fig. 4, these stationary (in-body coordinates) patterns might have very large peaks and yet be phased so as to pass through the dead zone at the angular position of the sensor. This potential difficulty is overcome by making  $J_s/J_n$  slightly different than 1.5, so that the three-lobed pattern revolves as shown in the figures. During acquisition, this departure from the ideal  $J_s/J_n$  ratio causes the periodic build-up and decay of nutation apparent in the simulation results.

Although a  $J_s/J_n$  ratio near 1.5 is more convenient for illustration because of the counter-rotating vectors in body coordinates, the same principles apply if  $J_s/J_n$  is 0.5. In this case, one-half nutation cycle is approximately one spin cycle. The detector is positioned near the torque axis, and the delay allows a full cycle of apparent target motion (opposite the spin direction) for the mean attitude error correction and

$180^\circ$  of difference rate rotation (also opposite the spin direction) for the nutation reduction mode.

#### Spin Rate Compensation

Because the position of the sensor axis relative to the torque axis is dependent only upon the vehicle moment of inertia ratio, variations in spin rate can be accommodated by adjusting the electrical delay time and torque pulse duration. If the design is based on a maximum spin rate, the correction for lower rates consists of: 1) reducing the torque pulse duration in proportion to spin rate to keep a fixed precession increment with the reduced angular momentum and 2) increasing the electrical delay time so that the total delay from target detection to the effective midpoint of the torque pulse is kept equal to one-half nutation cycle.

#### Analog Simulation

##### Description

The rotating vector model of apparent target motion in body coordinates leads to simple means of simulating the attitude behavior of a spinning vehicle with body-fixed sensor and torquer. Each of the rotating vectors is generated by a linear oscillator circuit as shown in the circuit diagram of Fig. 7. The outputs of the two oscillators are summed to give apparent target motion. For the data represented here, the sensor consisted of an X-Y plotter, with a metal disk replacing the pen, and a band of conducting paint representing the field of view. The electrical output from this device triggers a delay circuit that in turn triggers a pulse generator. The pulse length was set equal to  $90^\circ$  of vehicle rotation, requiring an electrical delay of  $180(1/1.55) - \frac{1}{2}(90) = 71^\circ$  of vehicle rotation for the case with  $J_s/J_n = 1.55$ . Because the body coordinate system is oriented to the torque axis, the precession rate appears only as a  $\beta$  input to the two oscillators. The output of the pulse generator is arranged to drive the  $\beta$  component of the  $h$  vector in the negative direction and the  $\beta$  component of the  $n$  vector in the positive direction. Response to body-fixed torques of any duration and waveform can be generated in this manner.

Changes in the  $J_s/J_n$  ratio are introduced by adjusting the frequency of the nutation oscillator. A third oscillator, operating at spin frequency, generates  $\sin \omega_s t$  and  $\cos \omega_s t$  for use in transforming the relative position of spin axis and target line of sight into inertial coordinates for display.

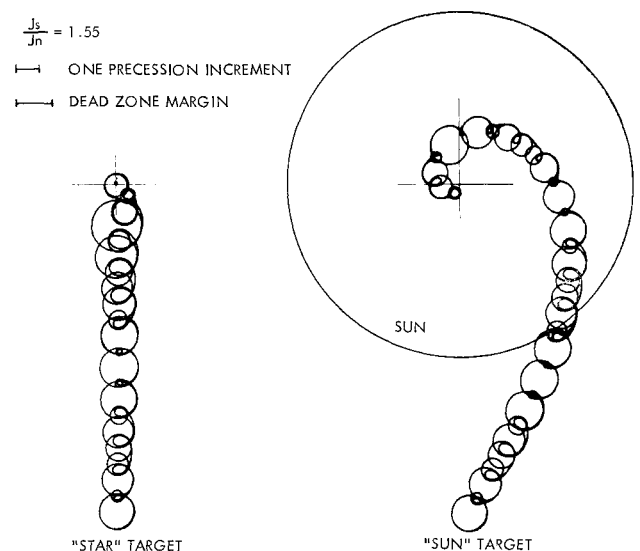


Fig. 8 Effect of target size on behavior.

## Results

Acquisition maneuver responses obtained with the analog simulation are shown in Fig. 8. Spin axis traces are shown for a point source target and one subtending an angle equal to 20 times the control system precession increment. In both cases, the final condition of the vehicle is a small residual nutation with its peak excursion within 1.5 precession increments (the dead-zone margin) of the target line of sight. The alternate growth and cancellation of nutation is exhibited with a low frequency "beat" effect introduced, because the moment-of-inertia ratio differs slightly from 1.5.

The large target causes the acquisition maneuver to follow a spiral path. The phase error that produces this effect is illustrated in Fig. 9, which shows the angular position of the target in body coordinates at the moment of detection. Mean attitude error is assumed to dominate nutation, so that apparent target motion is opposite the spin direction. When the required attitude correction is large, the phase error is equal to the target radius divided by the attitude error. As the acquisition maneuver proceeds, the phase error increases, reaching a maximum, as shown in Fig. 9, and then decreasing. The maximum phase error approaches a limit of  $90^\circ$  as the dead-zone margin is reduced relative to target size. Although this phase error does decrease the efficiency of the initial acquisition maneuver, the final tracking behavior of the control system is as good with a large target as with a point source.

The effect of initial nutation is illustrated by the time-history recordings in Fig. 10. The apparent target motion in body coordinates is shown, as well as its two components, mean attitude error and nutation. Initially, the system reduces the dominating mean attitude error until it is equal in magnitude to the nutation. Thereafter, both components of attitude error are reduced until apparent target motion lies within the dead-zone margin. In the particular case shown, the final condition was a small nutation clearly centered on the target.

## Laboratory Demonstration

The control system has also been demonstrated in the laboratory using the vehicle shown in Fig. 11. This vehicle has four independent channels with solenoid-valve-controlled torque jets at  $90^\circ$  intervals and four radial detector elements in the lead-sulfide detector of the sensor. The vehicle is supported on a three-degree-of-freedom spherical air bearing, with air for the spinup and torquing jets being drawn from

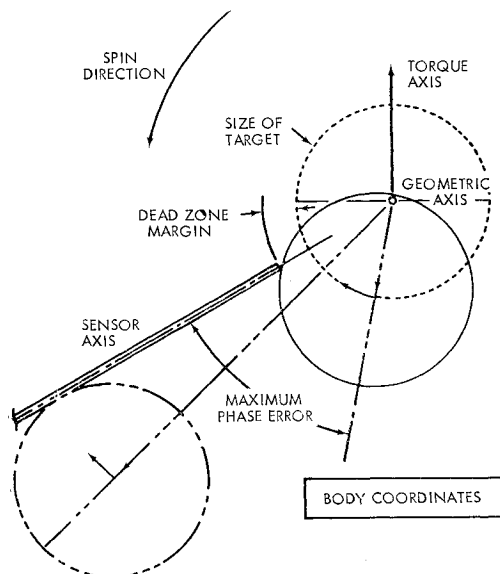


Fig. 9 Phase error due to target size.

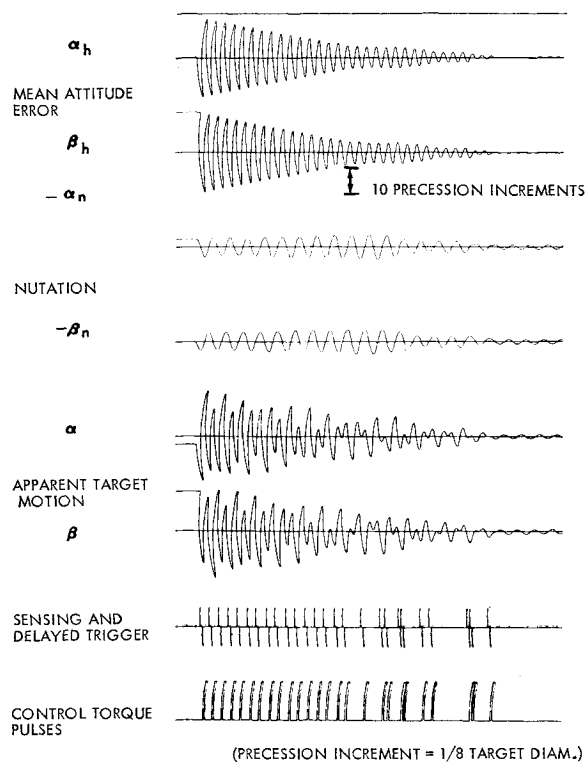


Fig. 10 Behavior with initial nutation.

the bearing supply by means of a hole through the vehicle-mounted sphere. Attitude response is measured optically.

Although this vehicle was designed to obtain qualitative data and no attempt was made to balance and align the components precisely, target tracking was demonstrated to an accuracy of  $1^\circ$ .

## Conclusions

The principal advantage of the control system described is its simplicity, promising lightweight and reliable mechanization. If delay time and pulse duration are compensated for spin rate, precise spin-rate regulation is not required. The target to which the vehicle spin axis is to be aligned can be of any angular size with no penalty in accuracy. The loss in efficiency due to phase error with a large target only affects the acquisition maneuver and, hence, may not be important in relation to the entire mission. Other phase errors due to nonideal operation can also be tolerated. Although efficient operation requires that the vehicle moment-of-inertia

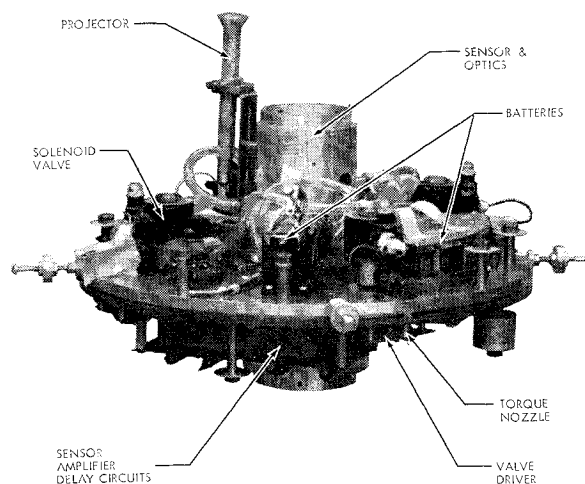


Fig. 11 Laboratory demonstrator.

ratio be constrained to regions near 0.5 or 1.5, these values are compatible with normal packaging designs.

### References

<sup>1</sup> Grubin, C., "A generalized two-impulse scheme for reorienting a spin-stabilized vehicle," ARS Preprint 1922-61 (1961).

<sup>2</sup> Garner, H. D. and Reid, H. J. E., Jr., "Simulator studies of simple attitude control for spin stabilized vehicles," NASA TN D-1395 (September 1962).

<sup>3</sup> Azeltine, J. A., *Transform Methods in Linear System Analysis* (McGraw-Hill Book Co., Inc., New York, 1958), 1st ed., Chap. 6, pp. 75-78.

NOVEMBER-DECEMBER 1964

J. SPACECRAFT

VOL. 1, NO. 6

## Missile Attitude Stabilization by Lyapunov's Second Method

ANTONY W. MERZ\*

*General Precision, Inc., Little Falls, N. J.*

A second-order version of a ballistic missile attitude-control system, with thrust gimbal deflection limiting, is examined. The exact stability boundaries are found, and a Lyapunov boundary is derived as a function of the system parameters. This boundary is identical to the exact boundary in the critical regions of the system phase plane. A third-order version, which includes gimbal dynamics, deflection limiting, and deflection rate limiting, is also analyzed. The exact boundaries in a portion of the phase space are found, and a means of determining the corresponding Lyapunov function by extending the second-order results is discussed.

### Nomenclature

$A, B$	= square symmetric matrices defining Lyapunov function
$a_i, b_i$	= elements of $A$ and $B$
$I$	= pitch axis moment of inertia, slug-ft <sup>2</sup>
$K_1$	= attitude loop gain, per rad
$K_2$	= rate gyro gain, per rad/sec
$K_3$	= inverse of actuator time constant, per sec
$l_\alpha$	= distance from c.g. to aerodynamic center, ft
$l_c$	= distance from c. g. to thrust gimbal point, ft
$m$	= vehicle mass, slugs
$N$	= normal force gradient, lb/rad
$s$	= Laplace transform operator, per sec
$T$	= thrust, lb
$U$	= vehicle velocity, fps
$V$	= Lyapunov function
$x$	= system state vector
$\alpha$	= angle of attack, rad
$\gamma$	= flight-path angle, rad
$\delta$	= gimbal deflection angle, rad
$\Delta$	= maximum value of gimbal deflection, rad
$\dot{\Delta}$	= maximum gimbal deflection rate, rad/sec
$\epsilon$	= command value of gimbal deflection, rad
$\eta$	= thrust vector control-system error signal, rad
$\theta$	= pitch attitude angle, rad
$\mu_c$	= $Tl_c/I$ , thrust moment effectiveness, rad/sec <sup>2</sup>
$\mu_\alpha$	= $Nl_\alpha/I$ , aerodynamic moment effectiveness, rad/sec <sup>2</sup>
$\omega$	= pitch rate, rad/sec

### Subscripts and superscripts

$A$	= amplitude-saturated region, $\delta = \pm \Delta$
$L$	= linear region
$R$	= rate-saturated region, $\dot{\delta} = \pm \dot{\Delta}$

Presented at the AIAA/ASD(AFSC) Vehicle Design and Propulsion Meeting, Dayton, Ohio, November 4-6, 1963 (no preprint number; published in bound volume of preprints of the meeting); revision received July 28, 1964. The author is grateful to P. C. Gregory, Head, Flight Control Department, and to B. Friedland, U. S. Air Force Aerospace Research Center, for their advice and suggestions during this investigation.

\* Staff Analyst. Member AIAA.

$LA$  = portion of amplitude-saturated region (see Fig. 7)  
 $RA$  = portion of amplitude-saturated region (see Fig. 7)  
 $( )^*$  = maximum value of Lyapunov constant guaranteeing system stability

### Introduction

THE present study is an application of the so-called second (or direct) method of Lyapunov to a simplified model of an unstable ballistic missile (see Fig. 1). The nonlinearities of the control system arise from the thrust vector control mechanism, which is considered to have a maximum amplitude ( $\pm \Delta$ ) and a maximum amplitude rate ( $\pm \dot{\Delta}$ ). Because of these nonlinear characteristics, no linear analysis techniques are applicable when either of the limits is reached.

The principle behind a stability analysis using Lyapunov's second method is the determination of a function  $V$  that is positive definite in a region surrounding the origin of the system state space. The sufficient condition for asymptotic stability is that the Lyapunov function be positive definite and that its derivative, which will incorporate the system equations of motion, be negative definite. References 1 and 2 provide the necessary background and discussion of the Lyapunov stability theory. In the analysis to follow, specific forms are assumed for the Lyapunov functions. These forms are

$$V = x^T A x + \int_0^\epsilon \delta(\epsilon) d\epsilon \quad (1)$$

for the second-order system and

$$V = x^T B x + \left( \frac{1}{K_3} \right) \int_0^\eta \dot{\delta}(\eta) d\eta \quad (2)$$

for the third-order system. In these expressions,  $x$  is the two- or three-dimensional state vector of the system and  $x^T$  is its transpose, as discussed in Ref. 3. The positive integral terms account for the saturation characteristics of the thrust vector actuator. These assumed forms for the Lyapunov